Lateral interactions in adsorbed layers

A. M. Bradshaw and M. Scheffler[a)]

Fritz-Haber-Institut der Max-Planck-Gesellschaft, Faradayweg 4-6, 1000 Berlin 33, West Germany

(Received 21 September 1978; accepted 19 December 1978)

Various mechanisms giving rise to attractive and repulsive forces between adspecies are considered. Such interactions can be classified as through-space (direct) or through-substrate (indirect), although a clear distinction is not possible. We describe in particular the interactions between both permanent and oscillating dipoles as well as those due to short-range overlap. The effect of these interactions on work function change, adsorption energy, UPS, and ir spectra are discussed. The adsorption systems Xe and CO/Pd(100) are used for the purposes of illustration.

PACS numbers: 68.20. + t, 79.60. − i, 82.65.My

I. INTRODUCTION

Although attention in recent years has focused on the chemical bond formed by an *isolated* atom or molecule with a metal surface, the lateral interactions in an adsorbed layer at finite coverages strongly influence the primary interaction with the surface and thus the energetics and structure of the adsorbate–metal system. By lateral interactions we mean the repulsive or attractive forces between adspecies which act in the surface plane. Examples of adsorption effects governed by lateral interactions are coverage-dependent changes in heat of adsorption and work function, order–disorder phenomena, and the migratory behavior of adspecies. The vibrational structure of adsorbed layers is also a two-dimensional problem, where the oscillators are coupled "mechanically" through the substrate as well as by their dynamic response to a radiation field. Lateral interactions may also affect the energetics and pathways of a catalytic reaction.[1] A possible classification of the phenomena would divide the fundamental mechanism into through-space (direct) and through-substrate (indirect)[2] (in loose analogy to the through-space and through-bond interactions in organic molecules, which have been discussed by Hoffmann[3]). Purely through-space effects are, however, difficult to isolate. Thus, the filled orbitals on neighboring chemisorbed species which overlap at small interadsorbate separations have acquired some metal character due to the interaction with the substrate. Similarly, a description of the repulsion of permanent dipoles must include the response of the metal conduction electrons. In the short description below of the interaction mechanisms we prefer to divide the effects according to the range of separation in which they are important for determining the net interaction energy.

Apart from the formation of ordered adlayers on single-crystal surfaces, probably the most important consequence of a repulsive lateral interaction between like species is a decrease in adsorption energy as a function of increasing coverage. A net *attractive* interaction involving favored neighboring sites invariably leads to island formation and to an initially constant adsorption energy. If the dependence of adsorption energy on coverage contains discontinuities dictated by lateral interactions then multiple peaks can arise in thermal desorption spectra.[4,5] Lateral interactions also change the charge distribution in adsorbed layers, a phenomenon which can be studied directly by measuring the change in work function. For an adsorbate-covered metal surface the latter is given by[6]

$$\Delta\phi = -4\pi n(qd - p) \tag{1}$$

where n is the adsorbate concentration, p the dipole moment of the adsorbed species perpendicular to the surface, q its net charge, and d the distance of q from the image plane. $2qd$ is thus the dipole moment of q and its image charge. We note in passing that the use of the classical concept of fictitious image charges is only approximately valid close to the surface.[7]

In the present article we discuss both long-range and short-range lateral interactions on metal surfaces and describe their effect on two model adsorption systems: Xe/Pd(100) and CO/Pd(100). Because of the absence of through-substrate chemical effects it is possible, at least qualitatively, to understand the changes in work function and heat of adsorption for physisorbed xenon. For the chemisorption of carbon monoxide the situation is more complicated and simple predictions as to charge distributions and energetics are not possible. We particularly lay emphasis on the manifestation of lateral interactions in vibrational and photoelectron spectroscopies. It is shown how short-range overlap effects can be observed in angular-resolved UPS. In vibrational spectroscopy of CO on metals we demonstrate that coverage-dependent shifts of the C–O stretch frequency are due mainly to dipole–dipole coupling and only to a lesser extent to bonding effects. The former is a dynamic lateral interaction occurring when the radiation field is switched on: it can be described with the same model used for describing the interactions between permanent dipoles.

II. THE MECHANISMS

A. Long-range forces

We consider initially those lateral interactions which play a role in the physisorption of rare gas atoms on a metal surface. Physisorption energies are typically 20–40 kJ mol^{-1} and the

 0022-5355/79/020447-08$01.00

bonding to the surface is due to attractive van der Waals forces roughly proportional to d^{-3}. These forces are ascribed to the collective motion of the electrons of the adatom and of the substrate. In terms of classical electrodynamics the metal forms instantaneous images of the fluctuating dipoles on the adatom, resulting in an attractive force. (Deviations from the classical concept arise when the metal conduction electrons no longer respond instantaneously to the adatom electrons, which then diminishes the importance of the interaction.[8,9] We do not discuss this problem here.) Due to the bonding interaction with the substrate the charge distribution on the adatoms is distorted and an electric multipole field is set up. For physisorption no net charge is found on the adatom (i.e. $q = 0$), a situation which pertains over the whole coverage range. Characteristic for the adsorption of rare gases on metal single crystal surfaces is also the formation of out-of-registry overlayers, from which it may be deduced that the *discrete* (atomic) structure[10] of the surface can be neglected in a first approximation. In the gas, liquid, and solid phases the interatomic forces are reasonably well understood.[11] They may be described in terms of pairwise interactions based on a potential such as the Lennard–Jones 6–12 function. The long-range part of this pair potential (r^{-6}) arises from a correlation of the motion of the electrons on different atoms and is again of the van der Waals type. (These forces are usually called London, or "dispersion" forces. The latter term is not to be confused with the dispersion discussed in Sec. II.B below). In the condensed phase three-body interactions are also important and in the case of xenon contribute 10% of the cohesive energy.[11] In the physisorbed phase, on the other hand, interaction mechanisms are present which are not found in the other phases.[12,13] These "new" repulsive forces are due to the interaction (both through-space and through-substrate) of permanent adatom multipoles induced by the adsorption process as well as to a three-body interaction (adspecies–substrate–adspecies) between fluctuating multipoles. At large separations these (repulsive) effects can be more important than the attractive part of the Lennard–Jones-type pair potential. Near the van der Waals minimum the interaction will become attractive. At still shorter range the interaction becomes strongly repulsive again (see Sec. II.B). This oscillatory behavior is superficially similar to that predicted by Einstein and Schrieffer[14] for through-substrate interactions in *chemisorbed* layers on a tight-binding solid. These authors show that, although the indirect pairwise interaction energy decays rapidly with separation, it is anisotropic and oscillatory in character. Using a reasonable choice of parameters the nearest-neighbor interaction is often found to be repulsive, while the next-nearest, third-nearest, or fourth-nearest is attractive. This would account for several commonly observed LEED patterns in chemisorbed overlayers such as $c(2 \times 2)$, $p(2 \times 2)$, and $c(4 \times 2)$. The neglect of short-range through-space overlap effects could, however, modify the quantitative conclusions. In general, the indirect interaction energy at nearest-neighbor separation is expected to be about one-tenth of the adsorption energy. In a simple MO picture of CO chemisorption Blyholder[15] also discusses the through-substrate lateral interaction and its effect on adsorption energy and C–O vibrational frequency.

We discuss now in more detail the multipole–multipole interactions because they can explain, at least for physisorption, the coverage-dependent work function changes. (In fact only dipole–dipole terms are considered; higher order multipoles can be neglected.) The dipole moment p on each atom as a function of coverage is given by

$$p(\theta) = p_{st} + \alpha E(\theta) \tag{2}$$

where p_{st} is the static dipole moment of the adparticle without the effect of screening by the metal conduction electrons, E is the component normal to the surface of the microscopic electric field at the dipole under consideration, and α is the polarizability of the adparticle. Using the classical concept of image dipoles and taking into account the permanent dipole fields of the other adspecies and images one obtains

$$E(\theta) = p(\theta)/4d^3 - p(\theta)[T(\theta) + V(\theta)] \tag{3}$$

where d is the distance to the effective image plane. The lattice sums T (the direct interaction) and V (the indirect interaction) are given by

$$T(\theta) = \sum_{\mathbf{R}_j}{}' \frac{1}{R_j^3} \tag{4}$$

$$V(\theta) = \sum_{\mathbf{R}_j}{}' \frac{1}{(R_j^2 + 4d^2)^{3/2}} - \frac{12d^2}{(R_j^2 + 4d^2)^{5/2}} \tag{5}$$

The $\mathbf{R}_j$ are the two-dimensional lattice vectors of the adlayer. Combining Eqs. (2) and (3) yields

$$p(\theta) = \frac{p_{st}}{1 + \alpha[T + V - 1/4d^3]}. \tag{6}$$

Due to the screening p_{st} is enhanced; its relation to the actual zero coverage dipole moment is given by

$$p(\theta = 0) = p_{st}/(1 - \alpha/4d^3). \tag{7}$$

Expressions similar to Eq. (6), but without the image terms, were proposed by Topping[16] and Miller.[17] More recently Antoniewicz[18] has derived a corresponding expression for two admolecules on the metal surface, where the molecules are represented by a positive charge and one harmonically bound negative charge. He also shows that for spherically symmetric adspecies there are no nonclassical (fluctuating dipole) contributions to Eq. (6); in anisotropic molecules, however, corrections could become important. Eq. (6) is expected to describe quite accurately the change in the induced dipole moment[19] and therefore, with the help of Eq. (1), the work function change as a function of coverage for a physisorbed layer.

In chemisorbed layers a quantitative description of the work function change is more complicated: firstly because of the nonclassical contributions and secondly because of the formation of a chemical bond between adspecies and substrate. The latter leads to a net charge q in Eq. (1), which is likely to vary as a function of coverage (see Blyholder, Ref. 15), as well as to a change in the polarizability of the adspecies.[20] However, the simple model which describes the change in work function in physisorption systems in terms of

dipole effects might also be a reasonable approximation for weak chemisorption systems up to moderate coverages.

An analysis of the change in heat of adsorption with coverage is somewhat more difficult because more terms must be considered and their energies evaluated. As well as two-body and three-body interactions via permanent multipoles there will be contributions from fluctuating (nonclassical) multipoles. The main contributions which would be included in a classical calculation of the change in adsorption energy are mentioned below in connection with the physisorption of Xe on Pd. In chemisorption the problem is rather different because the multipole phenomena are generally small in comparison to the through substrate chemical effects.

B. Short-range forces

At short range the pairwise interactions become repulsive due to the overlap of atomic or molecular wavefunctions on neighboring adspecies. This effect corresponds to the r^{-12} term in the Lennard–Jones potential and should become important when the adspecies separation is smaller than twice the van der Waals radius. In the discussion of this interaction we use the "surface molecule" concept, so that the overlapping wavefunctions may be considered as cluster wavefunctions, the cluster consisting of the adspecies and the metal atoms appropriate to the adsorption site. (In the example quoted below we will find, however, that the overlap effects can be reproduced reasonably well by treating simply an *isolated* monolayer.) When two such clusters "approach" each other as a consequence of increasing coverage, their wave functions will overlap, causing the formation of molecular-orbital-type eigenstates. One state will be symmetric with respect to the mirror plane between the clusters. This state will be bonding and have an energy lower than that of the cluster wave functions at large separation. The other state is antisymmetric, therefore antibonding and shifted to higher energy. Because the shift of the antibonding level is greater than that of the bonding level the total energy is increased and this type of interaction is repulsive *if both states are filled.* In the case of an ordered array of such clusters, the eigenstates become two-dimensional Bloch states $|n, \mathbf{k}_\parallel\rangle$, where n is the band index and $\mathbf{k}_\parallel$ a two-dimensional wave vector of the first surface Brillouin zone (SBZ) of the adlayer. Depending on the value of $\mathbf{k}_\parallel$ these states include wave functions which are symmetric with respect to neighboring clusters (thus bonding in the adlayer) and which give rise to the band minimum. There are also wave functions which are antisymmetric (antibonding) giving rise to the band maximum. Wave functions of lower symmetry will have an energy between these two values. With angular-resolved photoemission it is possible to map out this two-dimensional band structure and to obtain some indication of the coverage at which such overlap effects become important.

For the purposes of illustration it is useful to apply these ideas to an adsorbate layer in a quadratic structure (C_{4v} symmetry) such as the system $c(2 \times 2)$ Se/Ni(100). Taking p orbitals on the adsorbate atom suitably modified by the chemisorption bond to the substrate, group theory tells us that the cluster wavefunctions are of A_1 symmetry (p_z derived)

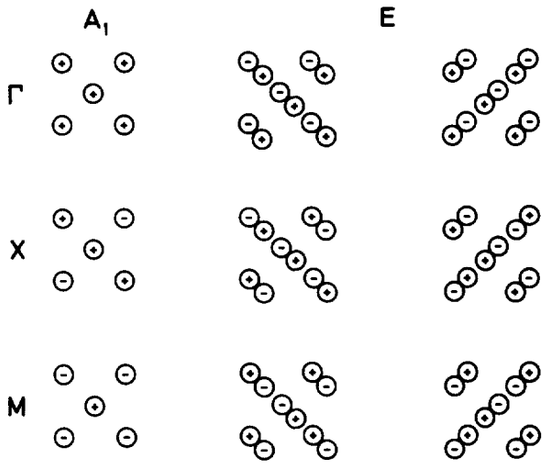

FIG. 1. Two-dimensional Bloch states (schematic) formed from localized wave functions belonging to representation A_1 (s or p_z derived) and belonging to representation $E(p_x,p_y$ derived) at the three high symmetry points of the SBZ of a quadratic array (see also insert in Fig. 2).

or of E symmetry (p_x, p_y derived). Figure 1 shows schematically the Bloch states constructed from such wave functions at the three high-symmetry points of the SBZ (see insert of Fig. 2):

$$\Gamma\colon \mathbf{k}_\parallel = (0,0);\ M\colon \mathbf{k}_\parallel = g/2(1,1);\ X\colon \mathbf{k}_\parallel = g/2(1,0)$$

where g is the length of the first two-dimensional reciprocal lattice vector of the adlayer. Figure 1 has been constructed using a simple tight-binding picture, i.e., by assuming that the Bloch states are described by

$$|n, \mathbf{k}_\parallel\rangle = \sum_{\mathbf{R}_j} e^{\mathbf{k}_\parallel \mathbf{R}_j}\, \phi_n\,(\mathbf{r} - \mathbf{R}_j) \qquad (8)$$

where the $\mathbf{R}_j$ are the lattice points of the adlayer and $\phi_n(\mathbf{r} - \mathbf{R}_j)$ is the a_1 state or an appropriate linear combination of the two degenerate e states. An analysis of Fig. 1 already yields the qualitative band structure: at Γ the a_1-derived two-dimensional Bloch state is completely bonding in the adlayer, whereas the e-derived states are mainly antibonding. Assuming a near degeneracy of the a_1 and e states in the isolated adsorbed atom, the overlap will push the e level to higher energy relative to the a_1 level. At M the a_1 level is antibonding and the e states are mainly bonding. At X the a_1-derived Bloch state is of mixed character. Because the X point has C_{2v} symmetry the degeneracy of the two e states will be lifted. One is completely bonding whereas the other is completely antibonding in the adlayer. For an isolated Se monolayer we have performed a simple tight-binding band structure calculation, which of course must show all these features (Fig. 2). The Se–Se spacing is taken as that in the $c(2 \times 2)$ Se–Ni(100) system and the necessary matrix elements are calculated numerically. Figure 2 also shows some band positions measured by Jacobi and von Muschwitz[21] using angular-resolved photoemission. The agreement is reasonably good, indicating that substrate effects are not very important in this case. This may not be true in general and the reader is referred to Liebsch[22] where the effect of the substrate is treated in detail.

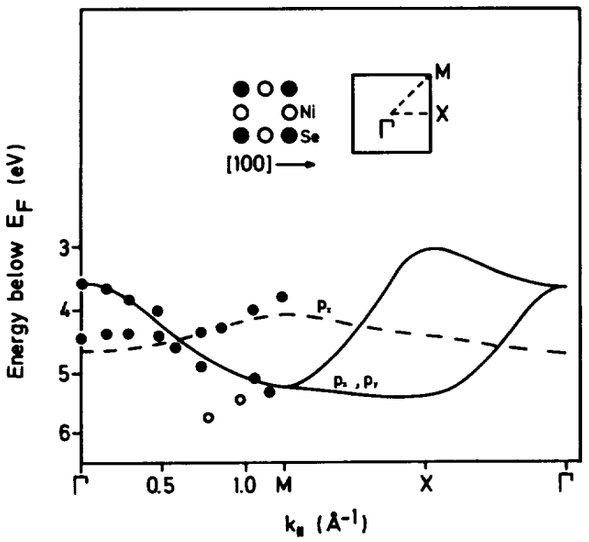

FIG. 2. Calculated band structure for an *isolated* monolayer of Se together with experimental results from Jacobi and v. Muschwitz.[21] The points represented by open circles are experimentally resolved only in the second SBZ and are attributed to substrate effects.

III. THE SYSTEM Xe/Pd(100)

To consider the effect of lateral interactions it is useful to study certain model systems which have been well characterized with a variety of measuring techniques. We have chosen the physisorption of xenon on Pd(100) as well as the molecular (associative) chemisorption of CO on the same surface. Because in a physisorbed system the interaction with the substrate is weak, it is easier to isolate multipole and overlap effects. The initial adsorption energy of xenon on Pd(100) is 33 kJ mol^{-1} decreasing to ~28 kJ mol^{-1} at maximum coverage.[23] The work function decreases nonlinearly with coverage to a value $\Delta\phi = -0.9$ eV.[23] Maximum coverage corresponds to the formation of an ordered hexagonal array out of registry with the substrate at $\theta = 0.44$ and can be characterized with LEED[23,24] and angular-resolved photoemission.[24] The Xe–Xe separation in the hexagonal layer is 4.48 Å compared to 4.34 Å in solid xenon.[25]

Figure 3 shows the measured change in work function (Palmberg[23]) compared to calculations using Eq. (3). For the separation of the Xe dipole and the image plane we use d = 1.5 Å, which is estimated from relaxation effects in UPS spectra.[26] For the polarizability the gas-phase value, $\alpha = 4$ Å^3 is used. For the hexagonal monolayer the lattice sums are calculated to be $T + V = 0.17$ Å^{-3}. The only remaining parameter is the dipole moment of a single adsorbed Xe atom $p(0)$. To give the best agreement between theory and experiment, this is determined to be 0.93 D with the positive end away from the surface. Palmberg[23] gives a value of 0.7 D, but neglects image charge screening effects and has to fit the polarizability to a value of 8 Å^3. Antoniewicz[27] calculates a value of 0.95 D. The problem of the interpolation of the lattice sums T and V between the limits of zero coverage and the monolayer has still to be discussed. If an ordered array is present at every coverage and only the lattice constant decreases, then the lattice sums should be proportional to $\theta^{3/2}$ (Topping[16]), whereas for a random distribution of adatoms they should be proportional to θ (Miller[17] and Mahan and Lucas[28]). In Figure 3 both curves are shown. Better agreement with experiment is obtained for the $\theta^{3/2}$ curve, although there is no real evidence for ordered arrays at low coverages. The differences between the curves are, however, quite small and more accurate measurements are probably necessary before a definite conclusion can be drawn. Nonetheless, we note that the work function change for this system is described well by Eq. (3) and that a reasonable value of 0.93 D for the dipole moment of a single Xe atom is obtained.

The decrease in heat of adsorption with coverage, which in the limits of experimental error is found to be linear,[23] is shown in the upper part of Fig. 4. This indicates a net repulsive long-range interaction in the layer, which is apparently not the case for Xe/Ag(111).[25,29] The change in adsorption energy is due to direct and indirect (through-substrate) interactions via fluctuating as well as via permanent dipoles. It is relatively straightforward to quantify some of these interaction energies. The main problem is one of calculating the energy required to produce the permanent image dipole as well as estimating the through substrate interaction via fluctuating dipoles. For Xe/Pd(100) the other effects produce a net attractive interaction of 4.4 kJ mol^{-1} at the monolayer stage, which is obviously outweighed by the two unknown (repulsive) terms to produce the observed net repulsive interaction of 5 kJ mol^{-1}. In the case of Xe/Ag(111) the net interaction appears to be attractive at all coverages.[25,29]

An indication of the importance of interatomic overlap in the system Xe/Pd(100) is provided by the angular-resolved photoemission experiment.[24] We observe here not only the dispersion effects discussed above but also a partial lifting of the degeneracy of the $5p_{3/2}$ valence state due to the bonding interaction. At low coverages the spin-orbit split $5p_{1/2}$ and $5p_{3/2}$ levels are observed in the spectrum with the same separation as in the gas phase (1.3 eV); both peaks are, however, substantially broadened. On going to the hexagonal monolayer the spectrum at normal emission has the form shown in Fig

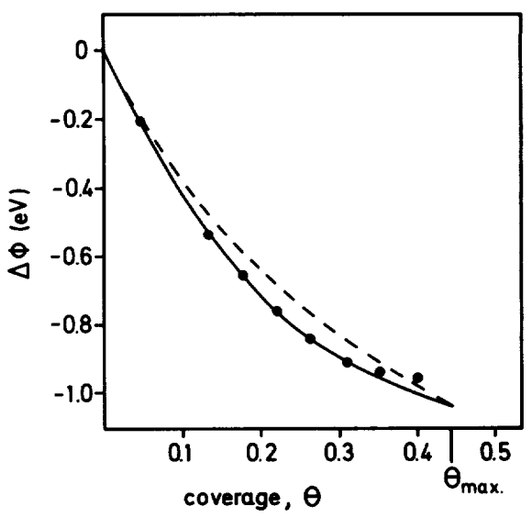

FIG. 3. Calculated work function change for Xe/Pd(100) as a function of coverage. Full line: lattice sums proportional to $\theta^{3/2}$, broken line: lattice sums proportional to θ. The points represent the experimental results of Palmberg.[23]

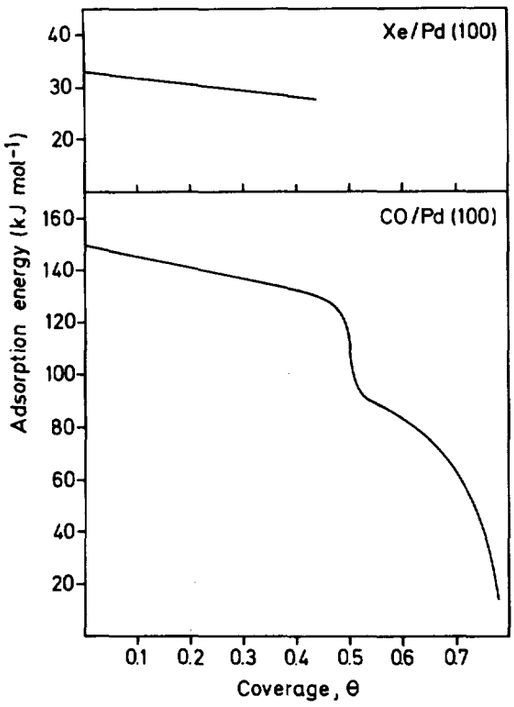

FIG. 4. The changes in heat of adsorption as a function of coverage in the systems Xe/Pd(100) and CO/Pd(100). After Palmberg,[23] Tracy and Palmberg,[31] and Bradshaw and Hoffmann.[32] Note the different energy scales.

5. The high ionization energy shoulders at 6.8 and 5.5 eV are attributed to a breakdown of $k_\parallel$ conservation, which is discussed in more detail elsewhere.[24] To explain the remaining features we consider the bonding scheme at the Γ point which is probed at normal emission ($k_\parallel = 0$, see also insert of Fig. 5). For the C_{6v} symmetry at the center of the SBZ there are only two-dimensional representations of the corresponding double group. The $p_{3/2}$ states will consequently show a twofold splitting in the xenon layer. As well as the $5p_{1/2}$ band there will thus be two bands derived from $5p_{3/2}$ states consisting of overlapping $m_j = \pm 1/2$ orbitals and of overlapping $m_j = +3/2$ orbitals. Constructing a two-dimensional Bloch function from an hexagonal array of $m_j = \pm 1/2$ orbitals, which have both p_z and p_x, p_y character, the resulting band consists of a mixture of bonding and antibonding contributions. The procedure is analogous to that described for the quadratic Se array in Sec. II.B. The $m_j = \pm 3/2$ orbitals are pure p_x, p_y in origin and lead to a $m_j = \pm 3/2$ band, which is entirely of antibonding character in the xenon layer. The $p_{3/2}$, $m_j = \pm 3/2$ derived Bloch state will therefore have the highest energy in the SBZ. Figure 5 shows the calculated band structure along the unique direction formed by the superposition of the two orthogonal domains of the hexagonal structure. (We call this direction ΓH; it corresponds to the [110] azimuth of the substrate). For the band structure only two-center integrals and nearest-neighbor interactions were taken into account; the $p_{3/2}$ and $p_{1/2}$ bands were calculated separately and matrix elements were evaluated numerically. The experimentally observed dispersion agrees well with the theory. At the Γ point we note that the midpoint between the $m_j = \pm 3/2$ and the $m_j = \pm 1/2$ bands is 1.5 eV higher in energy than the $p_{1/2}$ band. This is also true along ΓM and ΓK.[24] Since the separation before the splitting is only 1.3 eV, as in the gas phase, we are seeing here directly the repulsive nature of the interaction.

Because the $5p_{3/2}$, $m_j = \pm 3/2$ feature at 4.6 eV is very weak at normal exit, it is useful to investigate the coverage dependence of the splitting away from the Γ point where its intensity is greater. Such measurements[30] show that the splitting first becomes apparent at a coverage between 0.30 and 0.35. The first signs of extra features in LEED also occur around this coverage, although they are extremely diffuse and not definable. Sharp extra features are first obtained at the monolayer stage. The observation of ordering below the monolayer is probably due to the increasing restrictions on the movement of xenon atoms in the two-dimensional gas as its pressure is raised. Because of the largely repulsive long-range interactions and the shallow van der Waals minimum, it is unlikely that an island growth mechanism occurs in the layer. The observation of the splitting is, however, a measure of the coverage at which the short-range repulsion comes into play. It is of course independent of the formation of a hexagonal structure and occurs in any low symmetry configuration where the interatomic separation is small enough for overlap effects to play a role.

IV. THE SYSTEM CO/Pd(100)

At low coverages carbon monoxide on palladium (100) forms a disordered layer which Tracy and Palmberg[31] refer to as a random lattice gas. Just below $\theta = 0.5$ an ordering process takes place, resulting in sharp extra features from the two orthogonal domains of a $c(4 \times 2)R45°$ superstructure at

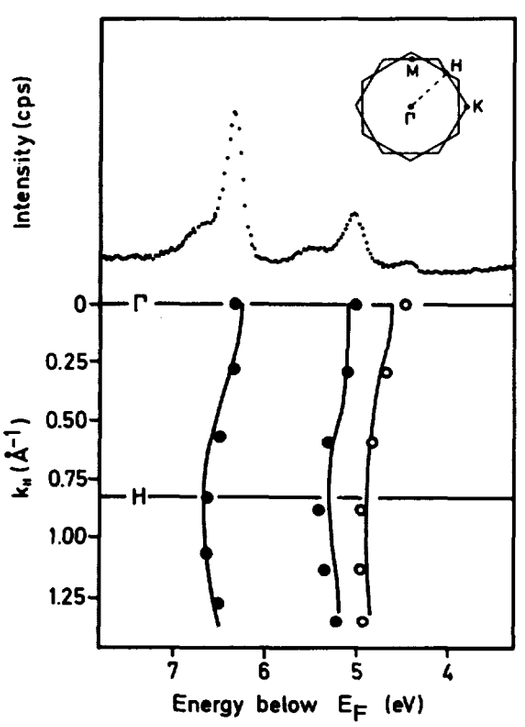

FIG. 5. He I UPS spectrum from a hexagonal xenon monolayer on Pd(100) at normal emission. Below: calculated two-dimensional band structure with experimental points.[24]

exactly half-coverage. At higher coverages the unit cell of the overlayer is continually compressed, the direction of compression being parallel to the [110] azimuths of the crystal. The half-coverage condition is characterized by a work function increase of 0.74 eV.[31] Because it is difficult to measure the coverage dependence of $\Delta\phi$ with any accuracy (for xenon this was possible with Auger spectroscopy), it is not possible to determine whether Eq. (6) is still a sufficiently good approximation. We use it nevertheless to reproduce the observed magnitude of $\Delta\phi$ at $\theta = 0.5$ and thus to determine the dipole moment $p(0)$ associated with a single adsorbed CO molecule. With a distance between the CO dipole and the metal image plane of 0.96 Å, the lattice sums for the $c(4 \times 2)R45°$ structure are calculated to be $T + V = 0.24$ Å^{-3} [see Eqs. (4) and (5)]. For the polarizability we take the gas phase value $\alpha = 2.6$ Å^3, which is the appropriate value for CO standing perpendicular to the surface. The dipole moment for a single adsorbed molecule is then $p(0) = 0.81$ D with the negative end away from the surface.

As shown in the lower half of Fig. 4 the initial heat of chemisorption of CO on Pd(100) is 150 kJ mol^{-1} falling to ~126 kJ mol^{-1} near to half-coverage, at which point a sharp decrease to ~93 kJ mol^{-1} occurs.[31,32] The more recent measurements[32] of adsorption energy and CO stretch frequency (see below) indicate that the discontinuity at $\theta = 0.5$ is not associated with the ordering process, but rather with loss of registry with the substrate, which takes place as the compression begins. We have therefore to explain the strong repulsive effects leading to a decrease of ~24 kJ mol^{-1} between zero and half-coverage. It is immediately apparent from the size of the permanent dipole that multipole interactions will not be any larger than in the system Xe/Pd(100). The answer must lie in the repulsive nature of the chemical interaction via the substrate.[14] Blyholder[15] has given a qualitative description of this phenomenon as it affects CO chemisorption; it could also have some consequences for the interpretation of vibrational spectra and is discussed again below. The $c(4 \times 2)R45°$ structure is not a square array and there are two intermolecular separations: 4.34 and 3.89 Å, the latter in the [100] direction. Assuming that the repulsive interaction is restricted to nearest neighbors, is identical in both directions and can be summed pairwise, the repulsive energy between two molecules on neighboring sites is ~8 kJ mol^{-1}, which is of the same order of magnitude as the interaction energies estimated from order–disorder transitions in other chemisorption systems.[33,34]

As the coverage is increased, the 3.89 Å separation remains constant and the unit cell is compressed in one direction such that the other nearest neighbor separation is reduced to 3.11 Å at $\theta = 0.8$. This compression is accompanied by a further, increasingly rapid decrease in adsorption energy. It is tempting to ascribe this decrease to the effect of short-range overlap. The semiempirical intermolecular potential of Kihara[35] for oriented nitrogen molecules gives us some feeling for the extent of the short-range repulsive interaction between two CO molecules when their axes are parallel. The van der Waals minimum is expected at ~3.5 Å (this is also the distance of closest approach to the α form of solid CO, where the molecular axes are not quite parallel[36]). At 3.9 Å the repulsive part of the pair potential yields a value of 0.4 kJ mol^{-1} and at 3.1 Å still only 6 kJ mol^{-1}, which lead to pairwise summed interaction energies much smaller than the decrease in adsorption energy.[37] That over lap effects do play a role at these coverages has, however, been established with angular-resolved photoemission.[38] Figure 6 shows the dispersion of the 4σ peak at $\theta = 0.8$ in two directions of the SBZ. The upper curve shows the effect along ΓH (see insert), which is the unique direction formed by the superposition of the two orthogonal domains. The lower curve shows the dispersion along the superimposed directions ΓM and $\Gamma K'$. Because the band at Γ is entirely bonding, as in the case of the p_z-derived band in Se/Ni(100), a minimum is obtained. Dispersion effects on the 5σ and 1π orbitals are more difficult to isolate as the two bands overlap in the spectrum. At $\theta = 0.5$ no dispersion can be observed, at least not within the limits of experimental accuracy. In order to ascribe the strong decrease in adsorption energy above $\theta = 0.5$ to overlap effects, it is necessary to assume that the effective range of the short range forces are considerably increased compared to the gas phase. All valence orbitals, in particular 5σ, will acquire some metal character due to the chemisorption bond and it is reasonable to assume that the repulsive overlap effect is amplified by the through-substrate contribution.

Infrared reflection–absorption spectroscopy also reveals

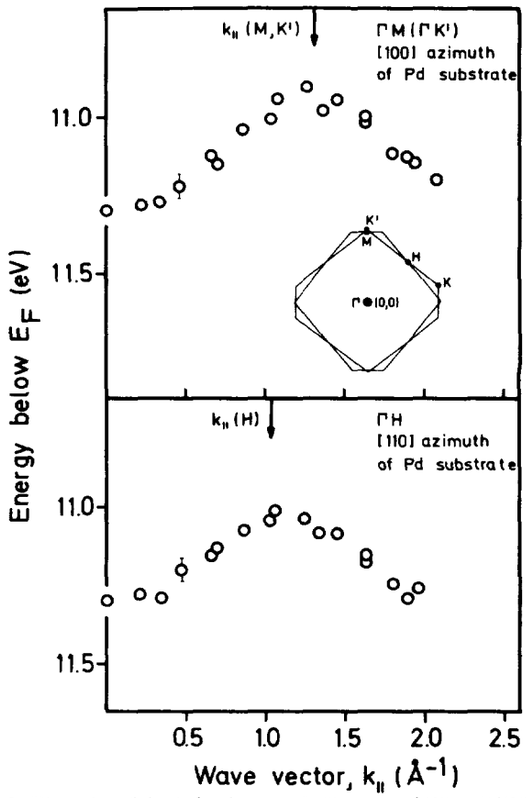

FIG. 6. Dispersion of the 4σ level in He II UPS spectra of CO on Pd(100) at 0.8 coverage. Above: The superimposed ΓM and $\Gamma K'$ directions where the edge of the SBZ is reached at $k_\parallel \sim 1.3$ Å^{-1} ($\theta_e = 31°$). Below: The unique ΓH direction where the edge of the SBZ is reached at $k_\parallel = 1.05$ Å^{-1} ($\theta_e = 24°$). The error bars indicated for one point on each curve apply of course to all points.

strong coverage-dependent effects. The spectrum from adsorbed CO shows an absorption band somewhat lower in frequency compared to the gas-phase C–O stretching mode (2143 cm^{-1}, 267.9 meV). With increasing coverage the band shifts to higher frequency. The phenomenon is quite general in CO chemisorption and is attributed by Blyholder[15] to the increased competition for metal electrons as the number of CO molecules on the surface increases. This decreases the extent of the interaction of metal electrons with the $2\pi^*$ orbital, increases the C–O stretch frequency and, as a further consequence, lowers the adsorption energy. An alternative explanation in terms of vibrational coupling (i.e., "mechanical" coupling between C–O nearest-neighbor oscillators via the substrate) has been offered by Moskovits and Hulse.[39] Using an approach based on Hammaker *et al.*[40] we have recently been able to show that dipole–dipole interactions can account for such shifts. The observed magnitude is, however, only reproduced by the theory when screening by the substrate is taken into account.[19]

That the C–O stretch frequency from adsorbed CO at low coverage is lower than in the gas phase (e.g., 1895 cm^{-1} in the system CO/Pd(100)[32]) is contrary to that expected from a purely mechanical model, where the metal–CO coupling should result in an increase of about 2.5% (~50 cm^{-1}). There are, however, further effects which lower the frequency. The interaction of the dipole field of the oscillating CO molecule with its own image dipole reduces the frequency by about 50 cm^{-1}.[19] Further, the C–O bond is expected to be weakened in the adsorbed phase due to the chemisorption bond.[15] The net reduction in the frequencies of the C–O stretching mode by ~150 cm^{-1} in the CO/Pd(100) system is thus qualitatively understood. We note in passing that in matrix-isolated CO, where image and chemical effects are not important but only a very weak CO-matrix bond of the van der Waal type exists, a small *increase* in frequency is observed.[41]

The lateral dipole–dipole interactions which can account for the observed coverage-dependent shifts can be treated with the same theory as that used above for the interpretation of work function data. Here we are dealing with oscillating dipoles which are excited by an external field rather than with permanent dipoles. The expression for the induced *oscillating* dipole is given by[19]:

$$p(\theta,\omega) = \frac{(1 + r_p)\,E^0}{1 + \alpha[T(\theta) + V(\theta) - 1/4d^3]} \qquad (9)$$

where E^0 and r_pE^0 are the incident field and the field reflected by the substrate at the CO molecule under consideration, respectively. α is the polarizability, which is essentially equal to the static one with an added Lorentzian term for the C–O resonance; d is, as before, the distance to the image plane; T and V are given by Eq. (5). In Fig. 7 we show the calculated change in the reflected intensity (Imp)[19] for CO on Pd(100) up to a coverage of $\theta = 0.5$, which is compared to the experimental results.[32] The polarizabilities are taken from the gas-phase and are treated as independent of coverage. The ir spectra[32] indicate that bridging positions are occupied in the coverage range up to $\theta = 0.5$. Different coverages $0 \leqslant \theta \leqslant 0.5$ are simulated by setting $T(\theta) + V(\theta) = F(\theta)T(0.5) + F(\theta)$-$V(0.5)$ with $0 \leqslant F(\theta) \leqslant 1$. The limits $F = 0$ and $F = 1$ correspond to the coverages $\theta = 0$ and $\theta = 0.5$. The exact relationship between F and θ is determined by the ensembles of different arrangements of neighboring molecules. The values of F are chosen here arbitrarily. The calculated shift between zero and half-coverage is, however, in good agreement with experiment. On top of this marked shift due to the dipole–dipole interaction there may also be a superimposed shift in the same direction due to the coverage-dependent interaction of the metal electrons with the CO $2\pi^*$ orbital.[15] However, as this latter effect appears to be associated with a decrease in binding energy in the CO/Pd(100) system, then a shift in the opposite direction is expected due to the reduced coupling of the CO moiety in the surface. Both effects would enter the theory by a coverage dependence of the vibrational part of the polarizability. The first contribution is not known numerically but the second contribution can be estimated within a purely mechanical model and would give a downward shift of the C–O stretch frequency by about 10 cm^{-1}. Due to the agreement obtained in Fig. 7 it would not seem unreasonable that these two additional effects are roughly of the same magnitude and therefore cancel, implying that α can be treated as independent of coverage as a first approximation. The similarity between the dependence of adsorption energy and C–O frequency on coverage thus appears to be largely coincidental. Both effects provide evidence for strong lateral interactions but the latter is mainly a dynamic effect associated with the radiation field required by the experiment.

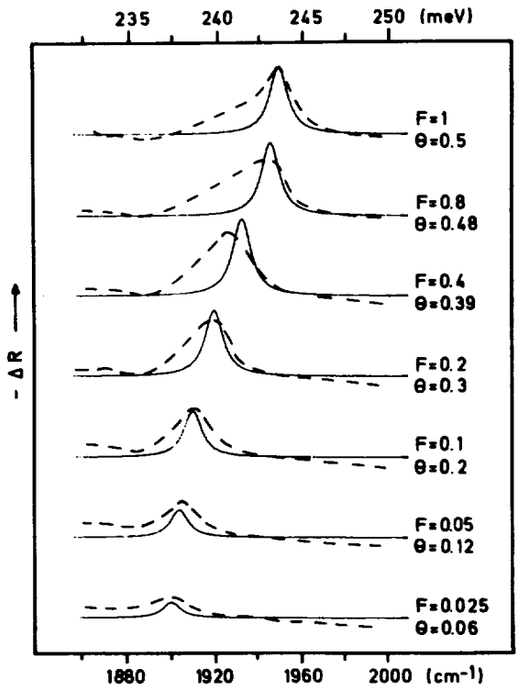

FIG. 7. Calculated change in the reflected intensity due to the adlayer for several coverages of CO on Pd(100) (full line, $F = 0.025 - 1$) together with experimental ir spectra from the C–O stretch region (dashed line, $\theta = 0.06 - 0.5$).[19,32]

ACKNOWLEDGMENTS

We acknowledge many useful discussions with our colleagues F. Hoffmann, K. Horn, K. Jacobi and K. Kambe.

[a]Present address: PTB, Gruppe 8.1, Bundesallee 100, 3300 Braunschweig, West Germany.
[1]T. Engel and G. Ertl. J. Chem. Phys. **69**, 1267 (1978).
[2]G. Ertl, J. Vac. Sci. Technol. **14**, 435 (1977).
[3]R. Hoffmann, Acc. Chem. Res. **4**, 1 (1971).
[4]D. A. King, Surf. Sci. **47**, 384 (1975).
[5]D. A. King, CRC Crit. Rev. Solid State Mater. Sci. 7(2) (1978) and references therein.
[6]N. D. Lang, Phys. Rev. B **4**, 4234 (1971).
[7]J. W. Gadzuk, in *Photoemission from Surfaces*, edited by B. Feuerbacher, B. Fitton, and R. F. Willis (Wiley, New York, 1978).
[8]J. Bardeen, Phys. Rev. **58**, 727 (1940).
[9]R. A. Pierotti and G. D. Halsey, J. Phys. Chem. **63**, 680 (1959).
[10]G. Ehrlich and F. G. Hudda, J. Chem. Phys. **30**, 493 (1959).
[11]e.g. J. A. Barker, R. O. Watts, J. K. Lee, T. P. Schaefer, and Y. T. Lee, J. Chem. Phys. **61**, 429 (1976).
[12]O. Sinanoglu and K. S. Pitzer, J. Chem. Phys. 332, 1279 (1960).
[13]A. D. McLachlan, Mol. Phys. **7**, 381 (1964).
[14]T. L. Einstein and J. R. Schrieffer, Phys. Rev. B **7**, 3629 (1973) and references therein.
[15]G. Blyholder, J. Phys. Chem. **68**, 2772 (1964).
[16]J. Topping, Proc. Roy. Soc. A **114**, 67 (1927).
[17]A. R. Miller, Proc. Camb. Phil. Soc. **42**, 292 (1946).
[18]P. R. Antoniewicz, Phys. Status solidi (b) **86**, 645 (1978).
[19]M. Scheffler, Surf. Sci, (in press).
[20]J. P. Muscat and D. M. Newns, J. Phys. C **7**, 2630 (1974).
[21]K. Jacobi and C. V. Muschwitz, Solid State Commun. **26**, 477 (1978).
[22]A. Liebsch, Phys. Rev. B **17**, 1653 (1978).
[23]P. W. Palmberg, Surf. Sci. **25**, 598 (1971).
[24]M. Scheffler, K. Horn, A. M. Bradshaw, and K. Kambe, Surf. Sci. **80**, 69 (1979).
[25]L. W. Bruch, P. I. Cohen, and M. B. Webb, Surf. Sci. **59**, 1 (1976).
[26]In UPS of xenon on Pd the Xe valence state peaks appear at about 2.4 eV higher energy than in the spectra from gas-phase or solid Xe. Assuming an additional relaxation mechanism for physisorbed Xe consisting exclusively of image charge screening ($\Delta E = e^2/4d$), we find $d = 1.5$ Å.
[27]P. R. Antoniewicz, Phys. Rev. Lett. **38**, 374 (1977).
[28]G. D. Mahan and A. A. Lucas, J. Chem. Phys. **68** 1345 (1978).
[29]G. McElhiney, H. Papp, and J. Pritchard, Surf. Sci. **54**, 617 (1976).
[30]K. Horn, M. Scheffler, and A. M. Bradshaw Phys. Rev. Lett. **41**, 822 (1978).
[31]J. C. Tracy and P. W. Palmberg, J. Chem. Phys. **51**, 4832 (1969); Surf. Sci. **14**, 274 (1969).
[32]A. M. Bradshaw and F. M. Hoffmann, Surf. Sci. **72**, 513 (1978).
[33]E. D. Williams, S. L. Cunningham, and W. H. Weinberg, J. Chem. Phys. **68**, 4688 (1978).
[34]J. Behm, K. Christmann, and G. Ertl. Solid State Commun. **25**, 763 (1978).
[35]T. Kihara and A. Koide, Adv. Chem. Phys. **33**, 52 (1975).
[36]R. W. G. Wyckoff, *Crystal Structures* (Wiley-Interscience, New York, 1963), 2nd ed., vol. 1.
[37]Palmberg and Tracy also noticed this discrepancy in Ref. 31. The difference here is further pronounced because of the anisotropic pair potential.
[38]K. Horn, A. M. Bradshaw, K. Hermann, and I. P. Batra (to be published).
[39]M. Moskovits and J. E. Hulse, Surf. Sci. **78**, 397 (1978).
[40]R. M. Hammaker, S. A. Francis and R. P. Eischens, Spectrochim. Acta **21**, 1295 (1965).
[41]J. B. Davies and H. E. Hallam, JCS Faraday II **68**, 509 (1972).